

# Quantum chemical study of $4f \rightarrow 5d$ excitations of trivalent lanthanide ions doped in the cubic elpasolite $\text{Cs}_2\text{NaYCl}_6$ . $\text{Ce}^{3+}$ to $\text{Tb}^{3+}$

Fernando Ruipérez

*Departamento de Química, C-XIV, Universidad Autónoma de Madrid, 28049 Madrid, Spain*

Zoila Barandiarán and Luis Seijo<sup>a)</sup>

*Departamento de Química, C-XIV, Universidad Autónoma de Madrid, 28049 Madrid, Spain*

*and Instituto Universitario de Ciencia de Materiales Nicolás Cabrera, Universidad Autónoma de Madrid, 28049 Madrid, Spain*

(Received 2 September 2005; accepted 24 October 2005; published online 23 December 2005)

Wave-function-based *ab initio* calculations on the lowest states of the  $4f^n, 4f^{n-1}5d(t_{2g})^1$ , and  $4f^{n-1}5d(e_g)^1$  configurations of  $(\text{LnCl}_6)^{3-}$  clusters ( $\text{Ln}=\text{Ce}$  to  $\text{Tb}$ ) embedded in the cubic elpasolite  $\text{Cs}_2\text{NaYCl}_6$  have been performed, in an attempt to contribute to a comprehensive understanding of the  $4f \rightarrow 5d$  excitations of lanthanide ions in crystals. Reliable data are provided on the changes of bond lengths and breathing mode vibrational frequencies upon  $4f \rightarrow 5d(t_{2g})$  and  $4f \rightarrow 5d(e_g)$  excitations, as well as on minimum-to-minimum and vertical absorption and emission transitions, and on the Stokes shifts. The available experimental data are discussed and predictions are made. The stabilization of the  $4f \rightarrow 5d(\text{baricenter})$  excitation of the doped ions with respect to the  $4f \rightarrow 5d$  excitations of the free ions, which is a key variable for the understanding of these excitations in solid hosts, is analyzed and found to be due, in two-thirds, to dynamic ligand correlation effects and, in one-third, to orbital relaxation, charge transfer, and covalency effects present in a mean-field approximation. © 2005 American Institute of Physics.  
[DOI: 10.1063/1.2137689]

## I. INTRODUCTION

The local states associated with the  $4f^{n-1}5d^1$  configurations of lanthanide ion impurities in ionic hosts are interesting from the technological and fundamental points of view. For instance, the spectral range and the high intensity of the  $5d \rightarrow 4f$  broad emission bands are interesting in phosphors, scintillators, and solid-state laser materials,<sup>1–4</sup> and the relative energies of the lowest states of the  $4f^{n-1}5d^1$  configurations and the highest of the  $4f^n$  configurations are relevant for the photon cascade emission of these systems, which is interesting for environmentally safe, Hg-free, short-wavelength Xe-discharge-based fluorescence lamps.<sup>5</sup> As examples of fundamental interest, accurate locations of the  $4f^{n-1}5d^1$  energy levels are essential for detailed calculations of intensities in processes where they act as intermediate states, such as electronic Raman scattering,<sup>4</sup> which are usually treated under energy-level baricenter approximations.<sup>6</sup> Also, the processes involved in the absorption and emission phenomena related to these states are not fully understood<sup>5,7</sup> and the understanding of nonradiative decay and other energy-transfer mechanisms that may involve electron-lattice coupling require the knowledge of the structure of the local defects in the excited  $4f^{n-1}5d^1$  manifolds, which is very difficult to obtain from the experiments alone.

*Ab initio* calculations are able to provide reliable data on the structure of the lanthanide ion defects in ionic crystals in their  $4f^{n-1}5d^1$  excited manifolds, as well as other informa-

tions and analyses that complement the experiments,<sup>8</sup> but it is only recently that they are beginning to appear in the literature.<sup>8–13</sup> In addition to having given interpretations of spectroscopic measurements in solid hosts doped with lanthanide and actinide ions,<sup>8,14–16</sup> and of energy-transfer mechanisms,<sup>15</sup> *ab initio* calculations have predicted the distance between *f*-element ions and their first coordination shell to shorten in the lowest  $4f \rightarrow 5d$  and  $5f \rightarrow 6d$  excitations of  $\text{Ce}^{3+}$ ,  $\text{Pr}^{3+}$ ,  $\text{Pa}^{4+}$ ,  $\text{U}^{3+}$ , and  $\text{U}^{4+}$  in sixfold chloride octahedral coordination<sup>8,14–16</sup> and of  $\text{Ce}^{3+}$  in eightfold fluoride cubic coordination.<sup>17</sup> This behavior, which contradicted the widespread assumption that bond length increases upon  $4f \rightarrow 5d$  and  $5f \rightarrow 6d$  excitations, has been found to be present in fluorides, chlorides, and bromides of  $\text{Ce}^{3+}$  in solid and liquid solutions.<sup>13</sup> The reasons behind it have been analyzed.<sup>11</sup> Also, it has been shown to be responsible for a predicted redshift of the lowest  $4f \leftrightarrow 5d$  transitions of  $\text{Cs}_2\text{NaYCl}_6:\text{Ce}^{3+}$  under high pressure, whose observation has been proposed as a simple alternative to time-resolved extended x-ray-absorption fine-structure (EXAFS) experiments for an experimental confirmation of bond-length shortening upon  $4f \rightarrow 5d$  excitation.<sup>18</sup>

Although *ab initio* calculations are expected to be useful in providing information that complements the experiments in a case by case basis, a comprehensive understanding of the  $4f \rightarrow 5d$  excitations of lanthanide ions in crystals (and  $5f \rightarrow 6d$  excitations of actinide ions as well) is convenient and necessary. In this respect, we may mention that remarkable correlations between a few hundred observed  $4f \rightarrow 5d$  excitations have been established by Dorenbos<sup>19–23</sup> which,

<sup>a)</sup> Author to whom correspondence should be addressed. Electronic mail: luis.seijo@uam.es

according to Bettinelli and Morcorgé,<sup>7</sup> can be rationalized on the basis of a model proposed by Judd<sup>24</sup> and Morrison<sup>25</sup> for the interactions between the induced dipole moment on the ligand and the electrons on the lanthanide. But, in spite of the rationalization power shown by the empirical model, its application faces a few problems. One of them is the availability of experimental data. For instance, the ligand field splittings of the  $5d$  orbitals of lanthanide ions are usually not known and strong assumptions have to be made in order to be able to deduce the transition energies from the  $4f$  baricenter to the  $5d$  baricenter; in fact, the lack of experimental data for the 10 Dq of lanthanide and actinide ions makes it usual to transfer experimental values of 10 Dq of  $\text{Ce}^{3+}$  ions to other lanthanide ions<sup>26</sup> and even to actinide ions.<sup>27</sup> Also, only transitions to the lowest high-spin state or to the lowest low-spin state of the  $4f^{n-1}5d^1$  configurations are usually observed, but not both, so diffculting the extraction of information on  $4f$ - $5d$  exchange interactions. Besides, experimental data are usually restricted to a few ions at the beginning of the series (and immediately after its first half) because the transition energies grow much with  $Z$  (they drop at the half shell) and become hard to measure as they overlap pure host absorptions/emissions. Finally, limitations to the validity of the Judd-Morrison model have been pointed out<sup>13</sup> and the development of improvements is desirable, which requires the availability of more reliable data.

In these circumstances, reliable and systematic *ab initio* results can be very helpful in establishing a comprehensive description of  $4f \rightarrow 5d$  excitations of lanthanide ions in crystals. In this paper, we present *ab initio* embedded cluster calculations on a series of  $(\text{LnCl}_6)^{3-}$  octahedral clusters ( $\text{Ln}=\text{Ce}$  to  $\text{Tb}$ ) in the cubic elpasolite  $\text{Cs}_2\text{NaYCl}_6$ . The performed calculations, which are wave-function based, consider host embedding effects of classical and quantum-mechanical nature on the clusters, and static and dynamic correlation and scalar relativistic effects within the embedded clusters; although spin-orbit effects are necessary in detailed spectroscopic studies, they are only of minor importance in all properties studied here and they have not been included. The reliability of the calculations of this kind has been shown before in specific studies on ionic hosts doped with  $\text{Ce}^{3+}$ ,  $\text{Pr}^{3+}$ ,  $\text{Pa}^{4+}$ ,  $\text{U}^{3+}$ , and  $\text{U}^{4+}$ .<sup>8,14-16</sup> We present results on the local structure of the defects in the ground  $4f^n$  state and in the lowest states of the  $4f^{n-1}5d(t_{2g})^1$  and  $4f^{n-1}5d(e_g)^1$  configurations of high and low spins. We calculated bond lengths, breathing mode vibrational frequencies, minimum-to-minimum energy differences, and vertical energy differences (including Stokes shifts). The results, which are an extension of a previous study on the ground states and lanthanide contraction of the same materials,<sup>12</sup> show the variation across the lanthanide series of the bond-length shortening upon  $4f \rightarrow 5d(t_{2g})$  excitation and bond-length enlargement upon  $4f \rightarrow 5d(e_g)$  excitation, the high-spin/low-spin energy differences, and the lowest  $4f \rightarrow 5d(t_{2g})$  and  $4f \rightarrow 5d(e_g)$  transition energies. We also present the lowest spin-allowed and spin-forbidden  $4f \rightarrow 5d$  transitions of the  $\text{Ln}^{3+}$  free ions, which are a necessary reference for discussion.

## II. METHOD AND DETAILS OF THE CALCULATIONS

Trivalent lanthanide ions  $\text{Ln}^{3+}$  doped in  $\text{Cs}_2\text{NaYCl}_6$  substitute for some of the  $\text{Y}^{3+}$  ions in the sites of exact octahedral ( $O_h$ ) symmetry, where they are surrounded by a first coordination shell of six  $\text{Cl}^-$  anions,<sup>28</sup> whose positions become directly affected by the presence of the lanthanide impurities. The electronic states of interest in this work are localized in the vicinities of the  $\text{Ln}^{3+}$  impurities ( $\text{Ln}=\text{Ce}$  to  $\text{Tb}$ ) and are expected to be well described with wave functions of  $(\text{LnCl}_6)^{3-}$ -embedded clusters. In the simplest description, they correspond to the  $4f^{n-1}5d^1$  open-shell configurations of the  $\text{Ln}^{3+}$  ions ( $n$  ranging from 1 in  $\text{Ce}$  to 8 in  $\text{Tb}$ ) and, in particular, to the  $(a_{2u}, t_{2u}, t_{1u})^{n-1}t_{2g}^1$  and  $(a_{2u}, t_{2u}, t_{1u})^{n-1}e_g^1$  configurations of  $(\text{LnCl}_6)^{3-}$ , where  $a_{2u}$ ,  $t_{2u}$ , and  $t_{1u}$  stand for the molecular orbitals (MOs) of  $(\text{LnCl}_6)^{3-}$  clusters with dominant character  $\text{Ln}^{3+}$ - $4f$  and  $t_{2g}$  and  $e_g$  for the MOs with dominant character  $\text{Ln}^{3+}$ - $5d$ ; the ligand field splittings are much larger in the  $5d$  orbitals than in the  $4f$  orbitals, which are shielded from the ligands and the rest of the environment by the  $5s$  and  $5p$  closed shells of  $\text{Ln}^{3+}$ . The ground states, which belong to the  $4f^n$  configurations, are included in the study for completeness.

All the local states of interest depend mainly on the intra-atomic interactions within  $\text{Ln}^{3+}$  and on the bonding interactions with the first coordination shell of  $\text{Cl}^-$ , but they also depend notably on the interactions between the  $(\text{LnCl}_6)^{3-}$  clusters and the rest of the host lattice. According to this hierarchy, we have chosen to perform high-quality wave-function-based molecular calculations on  $(\text{LnCl}_6)^{3-}$  clusters that are embedded in an approximate representation of the  $\text{Cs}_2\text{NaYCl}_6$  host. The embedding effects of the host on the cluster were included by means of an *ab initio* model potential<sup>29,30</sup> (AIMP) representation of the  $\text{Cs}_2\text{NaYCl}_6$  lattice, which was added to the Hamiltonian of the isolated cluster; it considers embedding interactions of electrostatic nature (Coulomb) and quantum-mechanical nature (host-cluster exchange and linear independence). The embedding AIMP were produced in Ref. 31 and correspond to the experimental crystal structure of  $\text{Cs}_2\text{NaYCl}_6$  [ $(O_h^5-F_{m3m})$ ,  $a=10.7396$  Å, and  $x_{\text{Cl}}=0.24393$ ].<sup>32</sup>

The calculations performed on the embedded cluster were state-average complete active space self-consistent-field (SA-CASSCF) calculations,<sup>33</sup> in order to describe the basic mean-field and nondynamical bonding interactions, and complete active space second-order perturbation-theory (CASPT2) calculations,<sup>34,35</sup> for the additional consideration of dynamic correlation effects. The complete active spaces corresponded to the distribution of  $n$  electrons ( $n=1-8$ ) in 13 MOs (the  $a_{2u}$ ,  $t_{2u}$ , and  $t_{1u}$  of main character  $\text{Ln}^{3+}$ - $4f$ , the  $t_{2g}$  and  $e_g$  of main character  $\text{Ln}^{3+}$ - $5d$ , and the  $a_{1g}$  of main character  $\text{Ln}^{3+}$ - $6s$ ). The CASSCF wave functions were considered to be the zeroth order for subsequent CASPT2 calculations where  $56+n$  electrons were correlated (the  $n$  open-shell electrons plus those in the MOs of main character  $\text{Ln}^{3+}$   $5s$  and  $5p$  and  $\text{Cl}^-$   $3s$  and  $3p$ ). Since many states are very close in energy, the multistate extension of the CASPT2 method was used (MS-CASPT2),<sup>36</sup> which is based on the multipartitioning quasidegenerate perturbation theory.<sup>37</sup> Be-

TABLE I. Ionization potential of the  $\text{Ln}^{3+}$  free ions (fourth ionization potential of the elements) computed with the spin-free Hamiltonian. All energies in eV.

	Initial state	Final state	CASSCF	MS-CASPT2	Expt. <sup>a</sup>	ACPF(g) <sup>b</sup>
Ce <sup>3+</sup>	$f^1(^2F)$	$p^6(^1S)$	40.32	35.79	36.76±0.01	35.60
Pr <sup>3+</sup>	$f^2(^3H)$	$f^1(^2F)$	37.23	38.23	38.98±0.02	38.40
Nd <sup>3+</sup>	$f^3(^4I)$	$f^2(^3H)$	38.87	40.05	40.4±0.4	40.08
Pm <sup>3+</sup>	$f^4(^5I)$	$f^3(^4I)$	39.14	40.73	41.1±0.6	40.64
Sm <sup>3+</sup>	$f^5(^6H)$	$f^4(^5I)$	39.33	41.14	41.4±0.7	41.12
Eu <sup>3+</sup>	$f^6(^7F)$	$f^5(^6H)$	40.98	42.79	42.7±0.6	42.55
Gd <sup>3+</sup>	$f^7(^8S)$	$f^6(^7F)$	42.57	44.77	44.0±0.7	44.31
Tb <sup>3+</sup>	$f^8(^7F)$	$f^7(^8S)$	35.83	38.35	39.37±0.10	38.44

<sup>a</sup>Reference 45.<sup>b</sup>After Cao and Dolg (Ref. 46). Performed with a basis set that includes up to  $g$  functions, as in this work, and spin-orbit corrections. The corrections for basis set limit are estimated by Cao and Dolg to range between 0.5 and 0.7 eV.

yond Nd<sup>3+</sup>, the use of a level shift operator<sup>38</sup> (followed by extrapolation to zero-level shift) was found necessary to achieve convergence of the MS-CASPT2 calculations.

We included scalar relativistic effects by means of relativistic effective core potentials, Cowan-Griffin-Wood-Boring AIMP.<sup>39,40</sup> For the lanthanides we used the [Kr] core AIMP ( $4d, 5s, 5p, 4f, 5d, 6s$  valence) and ( $14s10p10d8f$ ) valence Gaussian basis set of Ref. 41, augmented with one  $g$  polarization function obtained with a maximum radial overlap with the  $4f$  orbital, the final contraction being ( $14s10p10d8f3g$ )/[ $6s5p6d4f1g$ ]. For chlorine, we used the [Ne] core AIMP and valence Gaussian basis set of Ref. 40, augmented with one  $p$ -diffuse function for anions<sup>42</sup> and one  $d$ -polarization function,<sup>43</sup> the final contraction being ( $7s7p1d$ )/[ $3s4p1d$ ]. Additional basis set functions were located on the Na<sup>+</sup> ions next to the ( $\text{LnCl}_6$ )<sup>3-</sup> clusters; these are the ( $7s4p$ )/[ $1s1p$ ] contracted Gaussians which are the  $2s$  and  $2p$  orbitals of Na<sup>+</sup> embedded in Cs<sub>2</sub>NaYCl<sub>6</sub>,<sup>31</sup> which allow the achievement of a high degree of orthogonality between the cluster orbitals and the host orbitals and, so, enforce the host-cluster strong-orthogonality conditions implicit in the embedding method under use.<sup>30,44</sup> Spin-orbit coupling was not considered in this work.

### III. RESULTS AND DISCUSSION

#### A. Ln<sup>3+</sup> free ions

It is interesting to know the performance of the MS-CASPT2 method we used here for the very demanding  $f$ -ionization energies of the free ions, because the energy of an  $f \rightarrow d$  transition equals the difference between an  $f$ -ionization energy and a  $d$ -ionization energy, the former being much larger than the latter,  $\Delta E[f^n - SL \rightarrow f^{n-1}d^1 - S'L'] = \Delta E[f^n - SL \rightarrow f^{n-1} - S''L''] - \Delta E[f^{n-1}d^1 - S'L' \rightarrow f^{n-1} - S''L'']$ . In Table I we present the MS-CASPT2 results on the  $f$ -ionization potentials of the Ln<sup>3+</sup> free ions, together with the experiments<sup>45</sup> and average coupled-pair functional (ACPF) calculations of Cao and Dolg.<sup>46</sup> The present MS-CASPT2 calculations, as well as the ACPF calculations performed with a basis set including up to  $g$  functions, as in this work (note that Cao and Dolg<sup>46</sup> presented ACPF calculations including up to  $i$  functions and extrapolation to the basis set

limit), tend to underestimate the experiment, with the remarkable exception of Gd; we must note here that two different sources, very high quality *ab initio* calculations<sup>46</sup> and spectral hole burning experiments,<sup>47</sup> have suggested that the experimental fourth ionization potential of Gd needs a positive correction of 0.5–1 eV. The largest underestimations are in Ce, Pr, and Tb, where the experimental measurements are more precise. Basis set limit corrections to the ACPF calculations amount between 0.5 and 0.7 eV (Ref. 46) and spin-orbit effects should increase the  $f$ -ionization potentials some additional 0.3 eV; adding these corrections to the present MS-CASPT2 results would make us expect a final set of values with a systematic small overestimation, as is the case of the spin-orbit corrected ACPF calculations at the basis set limit.<sup>46</sup>

It is common to look at the  $4f \rightarrow 5d$  transitions in crystals as the result of a depression with respect to the corresponding free-ion transition<sup>7</sup> plus a splitting due to ligand field effects. Unfortunately, very few experimental data on the  $4f \rightarrow 5d$  excitations in free ions are available and sets of estimated values<sup>48,49</sup> have to be used.<sup>20</sup> In Table II we present our MS-CASPT2 results on the  $4f \rightarrow 5d$  excitation energies of the Ln<sup>3+</sup> free ions, which will serve as a reference for further discussion on the transitions of the Ln<sup>3+</sup>-doped ions, together with the available experimental data.<sup>45</sup> The lowest spin-allowed and spin-flip transitions are shown. The CASSCF results are also included in order to see the dynamic correlation effects on these transitions. The MS-CASPT2 calculations underestimate the experimental results available for Ce, Pr, and Tb; the underestimations are smaller here than for the  $4f$ -ionization energies and they might largely be due to basis set truncation effects and spin-orbit coupling. We expect these errors to be an upper limit of the errors found for the same ions in crystals, where the high angular momentum basis set functions are not as necessary as in the gas phase because of the presence of ligand basis set functions. It is interesting to observe that the  $5d$ -ionization potentials (computed as the difference between the  $4f$ -ionization potentials and the  $4f \rightarrow 5d$  excitation energies) rise smoothly from Ce<sup>3+</sup> to Gd<sup>3+</sup> (30.25, 30.99, 31.51, 31.94, 32.30, 32.71, and 32.94 eV), as a consequence of the increasing effective nuclear charge acting on the  $5d$  orbitals; a small



TABLE II.  $4f^n \rightarrow 4f^{n-1}5d^1$  transition energies of the  $\text{Ln}^{3+}$  free ions. All energies in  $\text{cm}^{-1}$ .

	Transition	CASSCF	MS-CASPT2	Expt. <sup>a</sup>
$\text{Ce}^{3+}$	$4f^{1-2}F \rightarrow 5d^{1-2}D$	43 580	44 670	49 940
$\text{Pr}^{3+}$	$4f^{2-3}H \rightarrow 4f^1 5d^{1-3}F$	56 310	58 380	62 070
	$4f^{2-3}H \rightarrow 4f^1 5d^{1-1}G$	54 370	56 480	58 730
$\text{Nd}^{3+}$	$4f^{3-4}I \rightarrow 4f^2 5d^{1-4}I$	66 440	68 890	
	$4f^{3-4}I \rightarrow 4f^2 5d^{1-2}H$	64 560	66 600	
$\text{Pm}^{3+}$	$4f^{4-5}I \rightarrow 4f^3 5d^{1-5}K$	65 520	70 880	
	$4f^{4-5}I \rightarrow 4f^3 5d^{1-3}I$	70 300	73 950	
$\text{Sm}^{3+}$	$4f^{5-6}H \rightarrow 4f^4 5d^{1-6}L$	63 580	71 290	
	$4f^{5-6}H \rightarrow 4f^4 5d^{1-4}H$	71 990	76 190	
$\text{Eu}^{3+}$	$4f^{6-7}F \rightarrow 4f^5 5d^{1-7}K$	74 080	81 340	
	$4f^{6-7}F \rightarrow 4f^5 5d^{1-5}F$	80 720	84 980	
$\text{Gd}^{3+}$	$4f^{7-8}S \rightarrow 4f^6 5d^{1-8}H$	88 490	95 397	
	$4f^{7-8}S \rightarrow 4f^6 5d^{1-6}P$	93 280	97 520	
$\text{Tb}^{3+}$	$4f^{8-7}F \rightarrow 4f^7 5d^{1-9}D$	29 780	45 080	50 610
	$4f^{8-7}F \rightarrow 4f^7 5d^{1-7}D$	43 110	51 730	60 870

<sup>a</sup>Landé averages of the experimental data from Ref. 45.

drop appears in  $\text{Tb}^{3+}$  (32.76 eV) marking the filling of the second half of the  $4f$  shell. It is this smooth  $Z$  dependence of the  $5d$ -ionization potentials that makes the variation of the  $4f \rightarrow 5d$  excitation energies across the series to be so similar to the variation of the  $4f$ -ionization energies (both in the gas phase and in the solid phase), as shown in Fig. 1.

### B. $(\text{LnCl}_6)^{3-}$ clusters embedded in $\text{Cs}_2\text{NaYCl}_6$

In Table III we show the computed bond lengths,  $R_e$ , and breathing mode harmonic vibrational frequencies,  $\omega_{a_{1g}}$ , of the  $(\text{LnCl}_6)^{3-}$  clusters embedded in  $\text{Cs}_2\text{NaYCl}_6$ , in the lowest states with main configurational characters  $4f^{n-1}5d(t_{2g})^1$  and  $4f^{n-1}5d(e_g)^1$  and maximum spin (high-spin states), and in the lowest states of the  $4f^{n-1}5d(t_{2g})^1$  configuration with the spin quantum number  $S$  reduced in one unit (low-spin or spin-flip states), together with those of the ground state of the  $4f^n$  configuration of Ref. 12. We also show the minimum-to-minimum excitation energies from the ground state,  $T_e$ .

The changes experienced upon excitation by the bond lengths between the lanthanide ions and the ligands are rep-

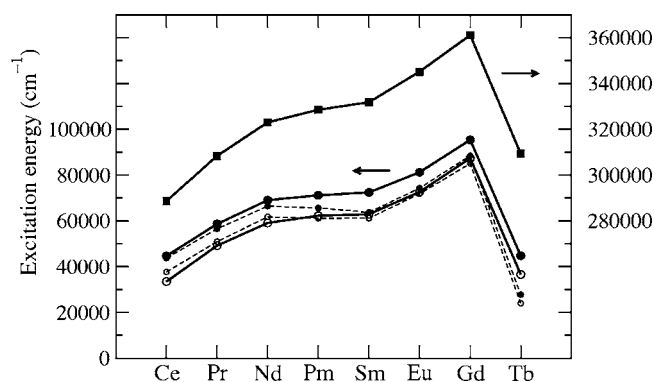


FIG. 1.  $4f \rightarrow 5d$  transition energies between the lowest states of high-spin (circles; left-hand vertical axis) and  $4f$  ionization energies (squares; right-hand vertical axis). Note that the left- and right-hand vertical scales are identical although shifted. Filled symbols:  $\text{Ln}^{3+}$  free ions. Open symbols  $4f \rightarrow 5d$ (baricenter) transitions of the  $\text{Ln}^{3+}$  ions doped in  $\text{Cs}_2\text{NaYCl}_6$ . Full lines: MS-CASPT2 results. Broken lines, CASSCF results.

resented in Fig. 2. It is clear that the bond lengths shorten upon  $4f \rightarrow 5d(t_{2g})$  excitation in all cases; parallelly, they lengthen upon the  $4f \rightarrow 5d(e_g)$  excitation in all cases. So, we can safely say that this behavior, which has been found before in  $\text{Ce}^{3+}$  and  $\text{Pr}^{3+}$  complexes,<sup>11</sup> is general in the lanthanide series. Out of the analyses of vibrational progressions, the absolute values of bond-length increments experienced in  $4f \rightarrow 5d(t_{2g})$  excitations have been estimated to be 0.050 Å in  $\text{Cs}_2\text{NaYCl}_6 \cdot (\text{CeCl}_6)^{3-}$  and 0.055 Å in  $\text{Cs}_2\text{NaYCl}_6 \cdot (\text{TbCl}_6)^{3-}$ .<sup>8,50</sup> We get 0.04 and 0.03 Å, respectively. In Fig. 2 we include the bond-length change upon excitation to the  $4f^{n-1}5d^1$  baricenter, where the effect of the ligand field splitting was approximately removed by a weighted average of the  $4f^{n-1}5d(t_{2g})^1$  states (weight 3/5) and the  $4f^{n-1}5d(e_g)^1$  states (weight 2/5). This change is negative and corresponds to a bond shortening of 0.02 Å, almost constant for the series. According to constraint space-orbital variation<sup>51,52</sup> (CSOV) analyses of mean-field CASSCF calculations performed in Ref. 11, this shortening is due to the fact that covalency and ligand-to- $4f$  charge transfer are larger in  $4f^{n-1}5d^1$  states than in the  $4f^n$  states; these effects tend to shorten the bonds upon excitation and they overcome a tendency to increase the bond length that is due to the larger size of the  $5d$  orbitals, which is, however, very small. (The reason why this tendency is very small, in spite of the fact that  $5d$  orbitals are much larger than the  $4f$  orbitals, can be understood with the help of an ionic model. According to it, it is the size of the outermost  $5s$  and  $5p$  filled shells that governs the bond lengths of the  $4f^n$  states and also the bond lengths of the  $4f^{n-1}5d^1$  states; in the latter case, the additional electron that occupies the more external  $5d$  shell slightly increases the distance.) A further bond-length shortening with respect to the  $4f^{n-1}5d^1$  baricenter is observed in the  $4f^{n-1}5d(t_{2g})^1$  states. This is an expected consequence of the ligand field effects, which make the  $5d(t_{2g})$  orbitals more stable than the  $5d$  baricenter, and the  $5d(e_g)$  less stable. The bond lengthenings of the  $4f^{n-1}5d(e_g)^1$  states with respect to the  $4f^{n-1}5d^1$  baricenter brought about by the ligand field ef-

TABLE III. MS-CASPT2 bond lengths  $R_e(\text{\AA})$ , breathing mode vibrational frequencies  $\omega_{a_{1g}}(\text{cm}^{-1})$ , and minimum-to-minimum energy differences  $T_e(\text{cm}^{-1})$  of the  $(\text{LnCl}_6)^{3-}$  clusters embedded in  $\text{Cs}_2\text{NaYCl}_6$ . The lowest states with a main character of the configurations  $4f^n$ ,  $4f^{n-1}5d(t_{2g})^1$ , and  $4f^{n-1}5d(e_g)^1$  and maximum spin quantum number  $S$  are shown. The baricenter entries correspond to weighted averages of the two latter states [weights 3 for the  $4f^{n-1}5d(t_{2g})^1$  configurations and 2 for the  $4f^{n-1}5d(e_g)^1$  configurations]. The lowest states of the  $4f^{n-1}5d(t_{2g})^1$  configurations with  $S$  reduced in one unit are shown as well. (a) First level of high  $4f^35d(e_g)^1$  character; it changes from 81% at  $R=2.54 \text{ \AA}$  to 87% at  $R=2.75 \text{ \AA}$ . (b) This level has a 99%  $4f^35d(e_g)^1$  character. (c) First level of high  $4f^45d(e_g)^1$  character; it changes from 45% at  $R=2.54 \text{ \AA}$  to 92% at  $R=2.75 \text{ \AA}$ . (d) This level has a 99%  $4f^45d(e_g)^1$  character.

$(\text{CeCl}_6)^{3-}$	$R_e$	$\omega_{a_{1g}}$	$T_e$	$(\text{SmCl}_6)^{3-}$	$R_e$	$\omega_{a_{1g}}$	$T_e$
$4f^1-1^2A_{2u}$	2.687	306	0	$4f^5-1^6T_{1u}$	2.633	309	0
$5d(t_{2g})^1-1^2T_{2g}$	2.645	307	24 295	$4f^45d(t_{2g})^1-1^6T_{2g}$	2.594	308	53 775
$5d(e_g)^1-1^2E_g$	2.705	300	47 219	$4f^45d(t_{2g}, e_g)^1-9^6T_{1g}$ (c)	2.648	233	76 587
$5d^1(\text{baricenter})$	2.669	304	33 465	$4f^45d(e_g)^1-5^6A_{2g}$ (d)	2.653	304	92 050
				$4f^45d^1(\text{baricenter})$	2.616	278	62 890
				$4f^45d(t_{2g})^1-1^4T_{2g}$	2.594	311	58 007
$(\text{PrCl}_6)^{3-}$	$R_e$	$\omega_{a_{1g}}$	$T_e$	$(\text{EuCl}_6)^{3-}$	$R_e$	$\omega_{a_{1g}}$	$T_e$
$4f^2-1^3T_{1g}$	2.670	304	0	$4f^6-1^7T_{1g}$	2.635	314	0
$4f^15d(t_{2g})^1-1^3T_{1u}$	2.626	305	39 892	$4f^55d(t_{2g})^1-1^7A_{2u}$	2.597	313	63 759
$4f^15d(e_g)^1-4^3T_{1u}$	2.690	299	62 998	$4f^55d(e_g)^1-4^7A_{2u}$	2.655	306	85 746
$4f^15d^1(\text{baricenter})$	2.651	303	49 134	$4f^55d^1(\text{baricenter})$	2.620	310	72 586
$4f^15d(t_{2g})^1-1^1A_{1u}$	2.628	305	37 529	$4f^55d(t_{2g})^1-1^5A_{2u}$	2.598	315	67 592
$(\text{NdCl}_6)^{3-}$	$R_e$	$\omega_{a_{1g}}$	$T_e$	$(\text{GdCl}_6)^{3-}$	$R_e$	$\omega_{a_{1g}}$	$T_e$
$4f^3-1^4A_{1u}$	2.660	307	0	$4f^7-1^8A_{1u}$	2.611	315	0
$4f^25d(t_{2g})^1-1^4E_g$	2.616	307	49 528	$4f^65d(t_{2g})^1-1^8T_{2g}$	2.573	316	78 283
$4f^25d(e_g)^1-3^4A_{1g}$	2.679	302	73 422	$4f^65d(e_g)^1-3^8T_{2g}$	2.632	308	100 949
$4f^25d^1(\text{baricenter})$	2.641	305	59 086	$4f^65d^1(\text{baricenter})$	2.597	313	87 349
$4f^25d(t_{2g})^1-1^2T_{1g}$	2.623	310	49 497	$4f^65d(t_{2g})^1-1^6T_{1g}$	2.564	317	80 868
$(\text{PmCl}_6)^{3-}$	$R_e$	$\omega_{a_{1g}}$	$T_e$	$(\text{TbCl}_6)^{3-}$	$R_e$	$\omega_{a_{1g}}$	$T_e$
$4f^4-1^5A_{1g}$	2.646	308	0	$4f^8-1^7A_{2g}$	2.597	312	0
$4f^35d(t_{2g})^1-1^5T_{1u}$	2.600	312	52 489	$4f^75d(t_{2g})^1-1^9T_{2u}$	2.568	317	28 302
$4f^35d(t_{2g}, e_g)^1-8^5E_u$ (a)	2.658	283	76 960	$4f^75d(e_g)^1-1^9E_u$	2.624	305	48 963
$4f^35d(e_g)^1-5^5A_{2u}^2$ (b)	2.663	301	91 190	$4f^75d^1(\text{baricenter})$	2.590	310	36 566
$4f^35d^1(\text{baricenter})$	2.623	300	62 277	$4f^75d(t_{2g})^1-1^7T_{2u}$	2.562	319	33 902
$4f^35d(t_{2g})^1-1^3T_{1u}$	2.605	310	55 265				

fects are large enough so as to make the final bond lengths to be longer in these states than in the  $4f^n$  ones.

The breathing mode vibrational frequencies in Table III show, in general, a very little change upon  $4f \rightarrow 5d(t_{2g})$  excitation and a small decrease upon  $4f \rightarrow 5d(e_g)$  excitation. In the cases of  $(\text{PmCl}_6)^{3-}$  and  $(\text{SmCl}_6)^{3-}$ , the start of the  $4f^{n-1}5d(e_g)^1$  manifold coincides in energy with a significant number of states of the  $4f^{n-1}5d(t_{2g})^1$  configuration; this results in a very large mixing of the two types of configurations, which depends very much on the Ln–Cl distance. As a result, the energy curves of the first states with a high character  $4f^{n-1}5d(e_g)^1$  are far from harmonic and the reported vibrational frequencies of the states  $8^5E_u$  of  $(\text{PmCl}_6)^{3-}$  and  $9^6T_{1g}$  of  $(\text{SmCl}_6)^{3-}$  are abnormally small and have a limited meaning. In order to show the effect of a  $4f \rightarrow 5d(e_g)$  excitation on the vibrational frequencies of  $(\text{PmCl}_6)^{3-}$  and  $(\text{SmCl}_6)^{3-}$ , we include in Table III the results on the states with a clearly dominant  $4f^{n-1}5d(e_g)^1$  character. They show the small decrease of vibrational frequency upon  $4f \rightarrow 5d(e_g)$  excitation.

There are a few experimental data on breathing mode

vibrational frequencies of  $4f^{n-1}5d^1$  levels of  $(\text{LnCl}_6)^{3-}$  moieties in  $\text{Cs}_2\text{NaYCl}_6$  in the literature. For  $\text{Cs}_2\text{NaYCl}_6:(\text{CeCl}_6)^{3-}$  in the  $5d(t_{2g})^1-2^2T_{2g}$   $\Gamma_{8g}$  level, the value of  $299 \pm 2 \text{ cm}^{-1}$  has been reported,<sup>8</sup> which does not differ from the  $4f^1$  ground configuration values in more than  $1 \text{ cm}^{-1}$  [ $300 \pm 2 \text{ cm}^{-1}$  in  $1 \Gamma_{8u}$ ,  $298 \pm 2 \text{ cm}^{-1}$  in  $1 \Gamma_{7u}$ , and  $299 \text{ cm}^{-1}$  in  $2 \Gamma_{8u}$  and  $2 \Gamma_{7u}$  (Ref. 8)]. Our spin-orbit-free result in  $5d(t_{2g})^1-2^2T_{2g}$ ,  $307 \text{ cm}^{-1}$ , is not far from the experiment and the fact that the  $4f^1$  and  $5d(t_{2g})^1$  configurations have an almost equal vibrational frequency is properly reproduced. For  $\text{Cs}_2\text{NaYCl}_6:(\text{TbCl}_6)^{3-}$  in its high-spin  $4f^75d(t_{2g})^1-9^9D \Gamma_{4u}$  and low-spin  $4f^75d(t_{2g})^1-7^7D \Gamma_{4u}$  levels, the respective values of  $297 \pm 2$  and  $298 \text{ cm}^{-1}$  have been reported.<sup>50</sup> The value in its ground  $4f^8$  configuration has not been measured, but  $290 \text{ cm}^{-1}$  is the known frequency in *neat*  $\text{Cs}_2\text{NaTbCl}_6:(\text{TbCl}_6)^{3-}$ ,<sup>50</sup> which has  $298 \pm 2 \text{ cm}^{-1}$  in the high-spin excited state, and a similar value can be assumed in  $\text{Cs}_2\text{NaYCl}_6:(\text{TbCl}_6)^{3-}$ . Our spin-orbit-free results in this case ( $312 \text{ cm}^{-1}$  in the ground state and  $317$  and  $319 \text{ cm}^{-1}$  in the high-spin and low-spin excited states) are again not far from the experiment. The facts that the frequency suffers a

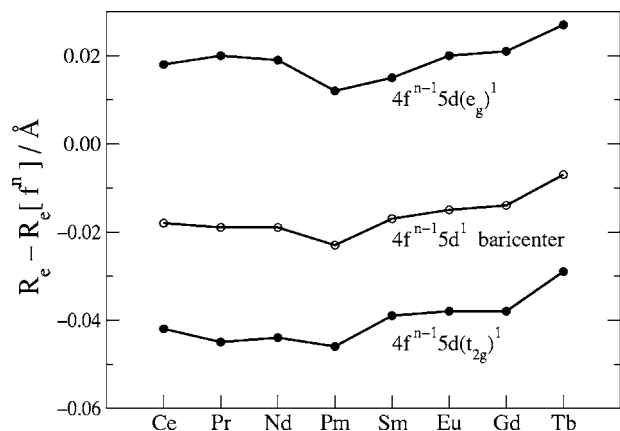


FIG. 2. Bond-length changes upon excitation from the lowest states of the  $4f^n$  configurations to the lowest states of the  $4f^{n-1}5d(t_{2g})^1$  and  $4f^{n-1}5d(e_g)^1$  configurations and their baricenters. MS-CASPT2 calculations.

small increase in the  $4f \rightarrow 5d(t_{2g})$  excitation and that it is almost equal in the high- and low-spin levels (slightly larger in the latter) are reproduced by the calculations. Looking at the results on  $Tb^{3+}$  and  $Ce^{3+}$  together, it is clear that the present calculations tend to overestimate the vibrational frequencies around 5%.

The minimum-to-minimum excitation energies from the ground state,  $T_e$ , grow from  $Ce^{3+}$  to  $Gd^{3+}$  and drop in  $Tb^{3+}$ , immediately after the half-filled  $4f$  shell. This is so for all the absorption transitions shown: to the high-spin  $4f^{n-1}5d(t_{2g})^1$  and  $4f^{n-1}5d(e_g)^1$  states (spin allowed from  $Ce^{3+}$  to  $Gd^{3+}$  and spin forbidden for  $Tb^{3+}$ ) and to the low-spin  $4f^{n-1}5d(t_{2g})^1$  states (spin forbidden from  $Ce^{3+}$  to  $Gd^{3+}$  and spin allowed for  $Tb^{3+}$ ). As we will see, several reasons make the variations of these transitions of the doped ions across the lanthanide series to be dominated by the variations of the free ions.

Firstly, the interplay between the  $4f$ - $5d$  Coulomb and exchange interactions and symmetry restrictions that is responsible for the relative stability of high-spin and low-spin states does not seem to be very different in the free ions and in the doped ions, in spite of the fact that the  $5d$  orbitals are very external and suffer the effects of the ligands strongly. This is clearly seen in Fig. 3, which shows the difference in total energies between the most stable low-spin (LS) and high-spin (HS) states of the  $4f^{n-1}5d^1$  configurations (free ions) and  $4f^{n-1}5d(t_{2g})^1$  configurations (doped ions). The largest difference between these effects from  $Pr^{3+}$  to  $Tb^{3+}$  amounts around  $7000\text{ cm}^{-1}$  and their impact on the variation of the transitions across the series should be small.

Secondly, the ligand field effects on the transitions are very much constant across the series. This can be seen in Fig. 3, where the difference between the energies of the lowest high-spin states of the  $4f^{n-1}5d(e_g)^1$  and  $4f^{n-1}5d(t_{2g})^1$  configurations is shown. The largest difference across the series is  $4000\text{ cm}^{-1}$ . It is interesting to remark that the very high energy of the states of the  $4f^{n-1}5d(e_g)^1$  configurations makes difficult their measurement in spectroscopical experiments, this resulting in a lack of experimental values of  $5d$  ligand field parameters for the lanthanide series. In these circumstances, it is a common practice to transfer experimental 10 Dq crystal-field parameters from  $Ce^{3+}$  ions to other lan-

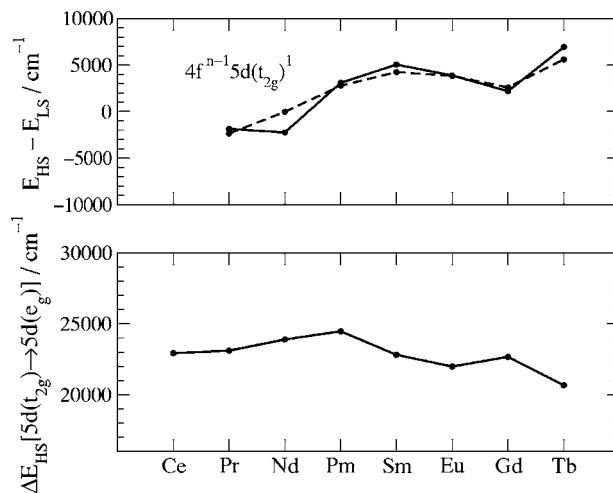


FIG. 3. Above: energy differences between the most stable low-spin (LS) and high-spin (HS) states of the  $4f^{n-1}5d^1$  configurations of  $Ln^{3+}$  free ions (dashed line) and of the  $4f^{n-1}5d(t_{2g})^1$  configurations of  $Ln^{3+}$  ions doped in  $Cs_2NaYCl_6$  (full line). The HS states have a maximum spin quantum number  $S$ ; the LS states have  $S-1$ . Below: energy differences between the lowest HS states of the  $4f^{n-1}5d(e_g)^1$  and  $4f^{n-1}5d(t_{2g})^1$  configurations of  $Ln^{3+}$  doped in  $Cs_2NaYCl_6$ . All numbers correspond to MS-CASPT2 calculations.

thanide ions<sup>26</sup> and, as a matter of fact, to actinide ions,<sup>27</sup> on the assumption that they would not change very much across the series. The present *ab initio* calculations provide a support for this practice within the lanthanide series.

Finally, the stabilization of the  $4f^{n-1}5d^1$  baricenter states of the  $Ln^{3+}$  ions doped in  $Cs_2NaYCl_6$  with respect to the  $4f^{n-1}5d^1$  states of the free ions (taking as a reference the ground  $4f^n$  states in all cases), which is shown in Fig. 4 together with the reduction experienced by the lowest  $4f \rightarrow 5d(t_{2g})$  transitions with respect to that of the free ions, is also quite constant across the series. This stabilization or, in other words, the reduction experienced by the  $4f \rightarrow 5d$  (baricenter) excitation of a  $Ln^{3+}$  free ion when it is introduced in a solid host, has been observed and analyzed by Dorenbos<sup>19-23</sup> in a large number of crystals containing  $Ce^{3+}$

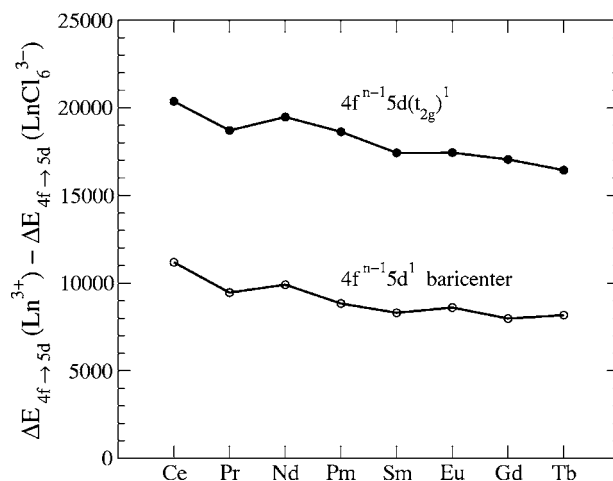


FIG. 4. Reduction experienced by the  $4f \rightarrow 5d$  transition energies of the  $Ln^{3+}$  free ions when they are doped in the chloroelpasolite  $Cs_2NaYCl_6$ . Open circles: transitions to the  $4f^{n-1}5d^1$  baricenters. Full circles: transitions to the lowest states with a maximum spin of the  $4f^{n-1}5d(t_{2g})^1$  configurations. MS-CASPT2 calculations.

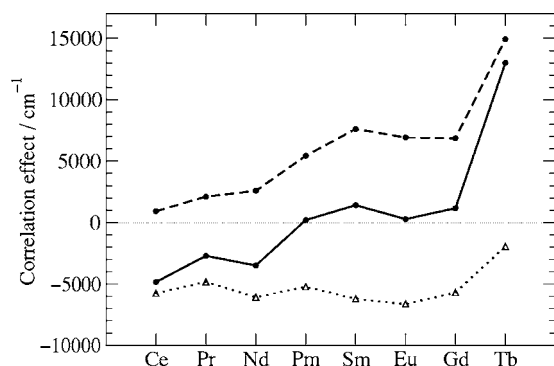


FIG. 5. Effects of dynamic correlation on the spin-allowed  $4f \rightarrow 5d(t_{2g})$  transition energies of  $\text{Ln}^{3+}$  ions doped in  $\text{Cs}_2\text{NaYCl}_6$  (full line), and on the spin-allowed  $4f \rightarrow 5d$  transition energies of  $\text{Ln}^{3+}$  free ions (dashed line), calculated as the difference between MS-CASPT2 and CASSCF results. Dotted line: ligand correlation effects estimated as the difference between the two lines above.

and  $\text{Pr}^{3+}$ , some containing  $\text{Nd}^{3+}$ , and a few containing  $\text{Sm}^{3+}$  and  $\text{Eu}^{3+}$ . Adopting reasonable assumptions, as that of using a common value of the crystal-field splitting for all the ions, he found the stabilization of the  $5d$  baricenter to be very similar for all the ions in a given host.

Since the previous effects are rather constant, specially the  $5d$  baricenter stabilizations and the crystal-field splittings, it is not strange that the variations of the  $4f \rightarrow 5d$  transitions of the  $\text{Ln}^{3+}$  ions doped in  $\text{Cs}_2\text{NaYCl}_6$  across the series resemble very much that of the free ions. The latter, as we justified above, is dominated by the variation across the series of the  $4f$ -ionization potentials. The results for the high-spin  $4f^{n-1}5d^1$  baricenter states are shown in Table III and Fig. 1, where they are plotted together with free-ion transitions and ionization potentials.

Let us come back to the stabilizations of the  $4f \rightarrow 5d$  transitions when the ions are introduced in a solid. Bettinelli and Morcorgé<sup>7</sup> suggested that they can be rationalized on the basis of a model proposed by Judd<sup>24</sup> and Morrison,<sup>25</sup> according to which this effect is dominated by the instantaneous interaction between the lanthanide's electron that is excited and the induced dipole moments on the ligands, which is different for  $4f$  and  $5d$  electrons due to their very different radial extensions. Consequently, the ligand polarizability is a key parameter of the model. This model has been successfully exploited by Dorenbos.<sup>19–23</sup> It is interesting to look at this interaction from the point of view of an *ab initio* calculation, where it can be associated with the dynamic correlation effects on the  $4f \rightarrow 5d$  transitions brought about by the ligands. We can compute it approximately in the following way. First, we compute the dynamic correlation effects on the  $4f \rightarrow 5d$  transitions of the  $(\text{LnCl}_6)^{3-}$  clusters embedded in  $\text{Cs}_2\text{NaYCl}_6$ , as the difference between the MS-CASPT2 results and the CASSCF results; then, we subtract from them the dynamic correlation effects on the  $4f \rightarrow 5d$  transitions of the free ions computed in the same way. The result is the ligand effects on dynamic correlation, on the assumption of additivity of ion and ligand correlation effects. The results are presented in Fig. 5. We can observe that the ligand correlation effects stabilize the  $4f \rightarrow 5d$  transitions and they do it in a rather constant way across the series. However, this

stabilization roughly amounts around  $6000 \text{ cm}^{-1}$ , which is only two-thirds of the full stabilization experienced by the baricenter (around  $9000 \text{ cm}^{-1}$ , see Fig. 4). The remaining  $3000 \text{ cm}^{-1}$  must be due to other effects that are included in the calculations and change from the free ions to the embedded clusters, namely, orbital relaxation, charge transfer, and covalent effects, which are notably different in the  $5d$  and  $4f$  orbitals. A more detailed knowledge on the relative importance of these would require CSOV analyses.

It is also interesting to see in Fig. 5 that the correlation effects on the  $4f \rightarrow 5d$  transitions are negative in the first ions of the lanthanide series, almost negligible from  $\text{Pm}^{3+}$  to  $\text{Gd}^{3+}$ , and become positive later. This is a consequence of the combination of an ion correlation effect that is always positive and grows with  $Z$ , and a ligand correlation effect that is negative and only slightly variable with  $Z$ . This is understood having in mind that these are excitations of one electron from inner, compact  $4f$  orbitals, which lie inside the  $5s^2$  and  $5p^6$  closed shells, to outer  $5d$  orbitals, much more exposed to the ligands. So, *ion* correlation stabilizes more a  $4f$ - $4f$  pair than a  $4f$ - $5d$  pair, and, in consequence, its stabilization of the states of the  $4f^n$  configuration must be larger than that of the states of the  $4f^{n-1}5d^1$  configuration, resulting in a positive contribution to the  $4f \rightarrow 5d$  transitions. Besides, this effect must increase with the number of electrons  $4f$ . Parallely, *ligand* correlation stabilizes the  $5d$ -ligand pairs and, at the same time, its effect on a  $4f$ -ligand pair should be very small, because  $4f$  orbitals and ligand orbitals are in different regions of real space, so resulting in a negative contribution to the  $4f \rightarrow 5d$  transitions. This effect does not depend much on  $Z$  because the extension of the  $5d$  orbitals and the bond lengths do not change much across the series.

Our results on the vertical absorption and emission transitions, and the corresponding Stokes shifts, are shown in Table IV. The computed transition energies cannot be directly compared with the experiments because they are spin-orbit-free. In *ab initio* calculations, spin-orbit effects are known to increase the first  $4f \rightarrow 5d$  absorption in  $\text{Ce}^{3+}$ -doped  $\text{Cs}_2\text{NaYCl}_6$  around  $1000 \text{ cm}^{-1}$ ,<sup>8</sup> but it would be difficult to quantify now these effects in other ions. Spin-orbit *ab initio* calculations on these systems are under way in our laboratory. However, the Stokes shifts are not expected to depend significantly on spin-orbit coupling in the cases under study, because they depend on the bond lengths and vibrational frequencies, if the vibronic couplings are not very important, and spin-orbit coupling has only very minor effects on these properties. To illustrate this, let us remark that simple geometry arguments lead to the conclusion that the Stokes shift between two harmonic energy curves with an identical curvature or force constant,  $k$ , and different equilibrium distances,  $R_e$  and  $R'_e$ , is given by  $\Delta E_{\text{Stokes}} = k(R_e - R'_e)^2$ . All Stokes shifts in Table IV are very close, as a consequence of the fact that all vibrational frequencies (and force constants) on the one hand and all bond-length shifts on the other, are also very similar. Roughly speaking, we should expect the Stokes shifts to be proportional to the squares of the bond-length shifts and this is observed in our results. The slightly larger absolute value of the bond-length change upon excitation found in  $\text{Pm}^{3+}$  and the slightly smaller value found in



TABLE IV. MS-CASPT2 minimum-to-minimum absorption transitions ( $T_e$ ), vertical absorption and emission transitions ( $\Delta E_{\text{absorption}}$  and  $\Delta E_{\text{emission}}$ ), and Stokes shifts ( $\Delta E_{\text{absorption}} - \Delta E_{\text{emission}}$ ). All energies in  $\text{cm}^{-1}$ .

$\text{Ln}^{3+}$	Transition	$T_e$	$\Delta E_{\text{absorption}}$	$\Delta E_{\text{emission}}$	Stokes shift
$\text{Ce}^{3+}$	$4f^{1-2}A_{2u} \rightarrow 5d^{1-2}T_{2g}$	24 300	24 790	23 770	1020
$\text{Pr}^{3+}$	$4f^2-^3T_{1g} \rightarrow 4f^15d(t_{2g})^1-^3T_{1u}$	39 890	40 450	39 310	1140
	$4f^2-^3T_{1g} \rightarrow 4f^15d(t_{2g})^1-^1A_{1u}$	37 530	38 030	37 000	1030
$\text{Nd}^{3+}$	$4f^3-^4A_{1u} \rightarrow 4f^25d(t_{2g})^1-^4E_g$	49 530	50 090	48 940	1150
	$4f^3-^4A_{1u} \rightarrow 4f^25d(t_{2g})^1-^2T_{1g}$	49 500	49 910	49 070	840
$\text{Pm}^{3+}$	$4f^4-^5A_{1g} \rightarrow 4f^35d(t_{2g})^1-^5T_{1u}$	52 490	53 090	51 830	1260
	$4f^4-^5A_{1g} \rightarrow 4f^35d(t_{2g})^1-^3T_{1u}$	55 270	55 770	54 750	1020
$\text{Sm}^{3+}$	$4f^5-^6T_{1u} \rightarrow 4f^45d(t_{2g})^1-^6T_{2g}$	53 780	54 320	53 290	1030
	$4f^5-^6T_{1u} \rightarrow 4f^45d(t_{2g})^1-^4T_{2g}$	58 010	58 480	57 500	980
$\text{Eu}^{3+}$	$4f^6-^7T_{1g} \rightarrow 4f^55d(t_{2g})^1-^7A_{2u}$	63 760	64 190	63 290	900
	$4f^6-^7T_{1g} \rightarrow 4f^55d(t_{2g})^1-^5A_{2u}$	67 590	67 990	67 160	830
$\text{Gd}^{3+}$	$4f^7-^8A_{1u} \rightarrow 4f^65d(t_{2g})^1-^8T_{2g}$	78 280	78 850	77 950	900
	$4f^7-^8A_{1u} \rightarrow 4f^65d(t_{2g})^1-^6T_{1g}$	80 870	81 450	80 180	1270
$\text{Tb}^{3+}$	$4f^8-^7A_{2g} \rightarrow 4f^75d(t_{2g})^1-^9T_{2u}$	28 300	28 740	28 190	550
	$4f^8-^7A_{2g} \rightarrow 4f^75d(t_{2g})^1-^7T_{2u}$	33 900	34 240	33 530	710

$\text{Tb}^{3+}$  are also seen in the Stokes shifts. The ratio between the squares of the bond-length change upon excitation of  $\text{Ce}^{3+}$  and  $\text{Tb}^{3+}$ , which is 2, is also seen in their respective Stokes shifts.

A few experimental data on Stokes shifts of these materials exist. The measurements of Tanner *et al.*<sup>8</sup> on the 10 K absorption spectrum of  $\text{Cs}_2\text{NaYCl}_6:\text{Ce}^{3+}$  have shown the maximum of the  $^2F_{5/2}\Gamma_{7u} \rightarrow ^2T_{2g}\Gamma_{7g}$  band around  $28\,800\text{ cm}^{-1}$  and its corresponding emission around  $27\,200\text{ cm}^{-1}$ ; this gives a Stokes shift of around  $1600\text{ cm}^{-1}$ , which is underestimated by our result of  $1020\text{ cm}^{-1}$ . This result is consistent with the experimental estimate of  $0.050\text{ \AA}$  for the absolute value of the bond-length change that accompanies this transition<sup>8</sup> and our calculation of  $-0.042\text{ \AA}$ . In the case of  $\text{Cs}_2\text{NaYCl}_6:\text{Pr}^{3+}$ , the 77 K emission spectrum of Laroche *et al.*<sup>53</sup> shows four bands with the lowest one extending from  $37\,000$  to  $39\,000\text{ cm}^{-1}$ , with its maximum at approximately  $38\,000\text{ cm}^{-1}$ ; their absorption spectrum shows a big intense band with multiple origins starting at  $38\,500\text{ cm}^{-1}$  and ending at  $45\,000\text{ cm}^{-1}$ , so that, although it is not absolutely clear in Ref. 53, it is reasonable to assume that the first absorption band maximum is around  $40\,000\text{ cm}^{-1}$ ; this would give an estimated Stokes shift of around  $2000\text{ cm}^{-1}$  if the absorption and emission corresponded to the same electronic transition; but, in the  $f^2 \rightarrow f^1d(t_{2g})^1$  case, the first electric dipole-allowed absorption may not coincide with the first allowed emission [these are  $f^2-A_{1g} \rightarrow f^1d(t_{2g})^1-T_{1u}$  and  $f^1d(t_{2g})^1-E_u \rightarrow f^2-T_{1g}$  in  $\text{Cs}_2\text{ZrCl}_6:\text{U}^{4+}$  (Ref. 15)], which would give a true Stokes shift smaller than  $2000\text{ cm}^{-1}$ . Our value of  $1140\text{ cm}^{-1}$  probably means an underestimation, which must be the consequence of the underestimation of the bond-length distortion produced by the  $4f \rightarrow 5d(t_{2g})$  electronic transition. Ning *et al.*<sup>50</sup> have measured the 10 K  $4f \rightarrow 5d(t_{2g})$  absorption spectrum of  $\text{Cs}_2\text{NaYCl}_6:\text{Tb}^{3+}$ . They found a spin-allowed band starting at  $41\,380\text{ cm}^{-1}$  and ending at approximately  $43\,000\text{ cm}^{-1}$ , with its maximum around  $41\,700\text{ cm}^{-1}$ , and a spin-forbidden band extending from  $34\,330$  to  $36\,800\text{ cm}^{-1}$ , with its maximum around  $35\,000\text{ cm}^{-1}$ . The difference

between these two maxima,  $6700\text{ cm}^{-1}$ , is not far from our calculation of  $5500\text{ cm}^{-1}$ , having in mind that the spin-orbit coupling will be different, in principle, in the  $4f^75d(t_{2g})^1-^9T_{2u}$  and  $4f^75d(t_{2g})^1-^7T_{2u}$  states. We are not aware of any report on the  $5d(t_{2g}) \rightarrow 4f$  emission spectrum of  $\text{Cs}_2\text{NaYCl}_6:\text{Tb}^{3+}$ . According to our results and assuming that they underestimate the Stokes shift as in  $\text{Ce}^{3+}$  and  $\text{Pr}^{3+}$ , we can predict the spin-allowed and the spin-forbidden emission to originate, respectively, at  $1100\text{--}1200$  and  $900\text{--}1000\text{ cm}^{-1}$  above the corresponding absorptions.

#### IV. CONCLUSIONS

AIMP MS-CASPT2 calculations have been performed on the  $(\text{LnCl}_6)^{3-}$  clusters ( $\text{Ln}=\text{Ce}$  to  $\text{Tb}$ ) embedded in cubic  $\text{Cs}_2\text{NaYCl}_6$ , in an attempt to contribute from the point of view of *ab initio* calculations to a comprehensive understanding of the  $4f \rightarrow 5d$  excitations of lanthanide ions in crystals. Reliable data are provided on the bond lengths and breathing mode harmonic vibrational frequencies of the defects in  $4f^{n-1}5d(t_{2g})^1$  and  $4f^{n-1}5d(e_g)^1$  configurations, and on their changes upon  $4f \rightarrow 5d(t_{2g})$  and  $4f \rightarrow 5d(e_g)$  excitations. Vibrational frequencies seem to be 5% overestimated and they experience very small changes in the excitations. Bond-length shortening upon  $4f \rightarrow 5d(t_{2g})$  excitation and lengthening upon  $4f \rightarrow 5d(e_g)$  excitation are found in all cases. The effect of the ligand field on the excitations is found to be very constant in the series and the variation of the excitations of the ions in the solid host across the lanthanide series resembles very much that of the free ions, which is governed by the  $4f$ -ionization potential of the  $\text{Ln}^{3+}$  ions. The depression of the  $4f \rightarrow 5d$  (baricenter) transitions of the doped ions with respect to the  $4f \rightarrow 5d$  transitions of the free ions is due to dynamic ligand correlation effects (two-thirds) and to the effects of orbital relaxation, charge transfer, and covalency (one-third); the depression of the  $4f \rightarrow 5d(t_{2g})$  transitions has the additional large contribution of the specific ligand field stabilization of the  $5d(t_{2g})$  orbitals. Stokes shifts are computed as well. Their comparison with the scarce available



experimental data suggests the existence of a systematically small underestimation, which is a manifestation of systematically small underestimation of the bond-length change upon  $4f \rightarrow 5d(t_{2g})$  excitation.

## ACKNOWLEDGMENTS

We are grateful to Professor Peter A. Tanner (City University of Hong Kong) for providing us with his results on  $\text{Cs}_2\text{NaYCl}_6:\text{Tb}^{3+}$  prior to publication. This work was partly supported by a grant from Ministerio de Educación y Ciencia, Spain (Dirección General de Investigación BQU2002-01316). One of the authors (F.R.) acknowledges a fellowship from Ministerio de Educación y Ciencia, Spain (Beca de Proyecto BQU2002-01316).

- <sup>1</sup>J. Ehrlich, P. F. Moulton, and R. M. Osgood, Jr., *Opt. Lett.* **4**, 117 (1979).
- <sup>2</sup>M. Nikl, *Phys. Status Solidi A* **178**, 595 (2000).
- <sup>3</sup>V. N. Makhov, N. M. Khaidukov, N. Y. Kirikova, M. Kirm, J. C. Krupa, T. V. Ovarova, and G. Zimmerer, *J. Lumin.* **87**, 1005 (2000).
- <sup>4</sup>P. A. Tanner, C. S. K. Mak, and M. D. Faucher, *Chem. Phys. Lett.* **343**, 309 (2001).
- <sup>5</sup>I. Sokólska and S. Kück, *Chem. Phys.* **270**, 355 (2001).
- <sup>6</sup>B. R. Judd, *Operator Techniques in Atomic Spectroscopy* (Princeton University Press, Princeton, NJ, 1965).
- <sup>7</sup>M. Bettinelli and R. Moncorgé, *J. Lumin.* **92**, 287 (2001).
- <sup>8</sup>P. A. Tanner, C. S. K. Mak, N. M. Edelstein, K. M. Murdoch, G. Liu, J. Huang, L. Seijo, and Z. Barandiarán, *J. Am. Chem. Soc.* **125**, 13225 (2003).
- <sup>9</sup>M. Marsman, J. Andriessen, and C. W. E. van Eijk, *Phys. Rev. B* **61**, 16477 (2000).
- <sup>10</sup>P. Dorenbos, J. Andriessen, and C. W. E. van Eijk, *J. Solid State Chem.* **171**, 133 (2003).
- <sup>11</sup>Z. Barandiarán and L. Seijo, *J. Chem. Phys.* **119**, 3785 (2003).
- <sup>12</sup>B. Ordejón, L. Seijo, and Z. Barandiarán, *J. Chem. Phys.* **119**, 6143 (2003).
- <sup>13</sup>Z. Barandiarán, N. M. Edelstein, B. Ordejón, F. Ruipérez, and L. Seijo, *J. Solid State Chem.* **178**, 464 (2005).
- <sup>14</sup>L. Seijo and Z. Barandiarán, *J. Chem. Phys.* **115**, 5554 (2001).
- <sup>15</sup>Z. Barandiarán and L. Seijo, *J. Chem. Phys.* **118**, 7439 (2003).
- <sup>16</sup>L. Seijo and Z. Barandiarán, *J. Chem. Phys.* **118**, 5335 (2003).
- <sup>17</sup>Z. Barandiarán and L. Seijo, *Theor. Chem. Acc.* (in press).
- <sup>18</sup>F. Ruipérez, L. Seijo, and Z. Barandiarán, *J. Chem. Phys.* **122**, 234507 (2005).
- <sup>19</sup>P. Dorenbos, *J. Lumin.* **87–89**, 970 (2000).
- <sup>20</sup>P. Dorenbos, *J. Lumin.* **91**, 91 (2000).
- <sup>21</sup>P. Dorenbos, *Phys. Rev. B* **62**, 15640 (2000).
- <sup>22</sup>P. Dorenbos, *Phys. Rev. B* **62**, 15650 (2000).
- <sup>23</sup>P. Dorenbos, *Phys. Rev. B* **64**, 125117 (2001).
- <sup>24</sup>B. R. Judd, *Phys. Rev. Lett.* **39**, 242 (1977).
- <sup>25</sup>C. A. Morrison, *J. Chem. Phys.* **72**, 1001 (1980).
- <sup>26</sup>P. A. Tanner, *Top. Curr. Chem.* **241**, 167 (2004).
- <sup>27</sup>M. Karbowiak, *J. Phys. Chem. A* **109**, 3569 (2005).
- <sup>28</sup>L. R. Morss, M. Siegal, L. Stenger, and N. Edelstein, *Inorg. Chem.* **9**, 1771 (1970).
- <sup>29</sup>Z. Barandiarán and L. Seijo, *J. Chem. Phys.* **89**, 5739 (1988).
- <sup>30</sup>L. Seijo and Z. Barandiarán, in *Computational Chemistry: Reviews of Current Trends*, edited by J. Leszczyński (World Scientific, Singapore, 1999), Vol. 4, p. 55.
- <sup>31</sup>A. Al-Abdalla, Z. Barandiarán, L. Seijo, and R. Lindh, *J. Chem. Phys.* **108**, 2005 (1998).
- <sup>32</sup>C. Reber, H. U. Güdel, G. Meyer, T. Schleid, and C. A. Daul, *Inorg. Chem.* **28**, 3249 (1989).
- <sup>33</sup>B. O. Roos, P. R. Taylor, and P. E. M. Siegbahn, *Chem. Phys.* **48**, 157 (1980); P. E. M. Siegbahn, A. Heiberg, J. Almlöf, and B. O. Roos, *J. Chem. Phys.* **74**, 2384 (1981); P. Siegbahn, A. Heiberg, B. Roos, and B. Levy, *Phys. Scr.* **21**, 323 (1980).
- <sup>34</sup>K. Andersson, P.-Å. Malmqvist, B. O. Roos, A. J. Sadlej, and K. Wolinski, *J. Phys. Chem.* **94**, 5483 (1990).
- <sup>35</sup>K. Andersson, P.-Å. Malmqvist, and B. O. Roos, *J. Chem. Phys.* **96**, 1218 (1992).
- <sup>36</sup>J. Finley, P.-Å. Malmqvist, B. O. Roos, and L. Serrano-Andrés, *Chem. Phys. Lett.* **288**, 299 (1998).
- <sup>37</sup>A. Zaitsevskii and J. P. Malrieu, *Chem. Phys. Lett.* **223**, 597 (1995).
- <sup>38</sup>B. O. Roos and K. Andersson, *Chem. Phys. Lett.* **245**, 215 (1995).
- <sup>39</sup>S. Huzinaga, L. Seijo, Z. Barandiarán, and M. Klobukowski, *J. Chem. Phys.* **86**, 2132 (1987).
- <sup>40</sup>Z. Barandiarán and L. Seijo, *Can. J. Chem.* **70**, 409 (1992).
- <sup>41</sup>L. Seijo, Z. Barandiarán, and B. Ordejón, *Mol. Phys.* **101**, 73 (2003).
- <sup>42</sup>T. H. Dunning and P. J. Hay, in *Modern Theoretical Chemistry*, edited by H. F. Schaefer III (Plenum, New York, 1977).
- <sup>43</sup>J. Andzelm, M. Klobukowski, E. Radzio-Andzelm, Y. Sakai, and H. Tatewaki, *Gaussian Basis Sets for Molecular Calculations*, edited by S. Huzinaga (Elsevier, Amsterdam, 1984).
- <sup>44</sup>J. L. Pascual, L. Seijo, and Z. Barandiarán, *J. Chem. Phys.* **98**, 9715 (1993).
- <sup>45</sup>W. C. Martin, R. Zalubas, and L. Hagan, *Atomic Energy Levels-The Rare Earth Elements*, Natl. Bur. Stand. Ref. Data Ser., Natl. Bur. Stand. No. (U.S.) Circ. 60 (U.S. GPO, Washington, D. C., 1978).
- <sup>46</sup>X. Cao and M. Dolg, *Chem. Phys. Lett.* **349**, 489 (2001).
- <sup>47</sup>C. W. Thiel, Y. Sun, and R. L. Cone, *J. Mod. Opt.* **49**, 2399 (2002).
- <sup>48</sup>J. Sugar and J. Reader, *J. Chem. Phys.* **59**, 2083 (1973).
- <sup>49</sup>L. Brewer, in *Systematics and the Properties of the Lanthanides*, edited by S. P. Sinha (Reidel, Dordrecht, 1983), p. 17.
- <sup>50</sup>L. Ning, C. S. K. Mak, and P. A. Tanner, *Phys. Rev. B* **72**, 085127 (2005).
- <sup>51</sup>P. S. Bagus, K. Hermann, and C. W. Bauschlicher, *J. Chem. Phys.* **80**, 4378 (1984).
- <sup>52</sup>C. W. Bauschlicher and P. S. Bagus, *J. Chem. Phys.* **81**, 5889 (1984).
- <sup>53</sup>M. Laroche, M. Bettinelli, S. Girard, and R. Moncorgé, *Chem. Phys. Lett.* **311**, 167 (1999).